

Biominalisation performance of bacteria isolated from a landfill in China

RAJASEKAR, Adharsh, WILKINSON, Stephen, SEKAR, Raju, BRIDGE, Jonathan <<http://orcid.org/0000-0003-3717-519X>>, MEDINA-ROLDAN, Eduardo and MOY, Charles K.S

Available from Sheffield Hallam University Research Archive (SHURA) at:

<http://shura.shu.ac.uk/22438/>

This document is the author deposited version. You are advised to consult the publisher's version if you wish to cite from it.

Published version

RAJASEKAR, Adharsh, WILKINSON, Stephen, SEKAR, Raju, BRIDGE, Jonathan, MEDINA-ROLDAN, Eduardo and MOY, Charles K.S (2018). Biominalisation performance of bacteria isolated from a landfill in China. *Canadian Journal of Microbiology (CJM)*, 64 (12), 945-953.

Copyright and re-use policy

See <http://shura.shu.ac.uk/information.html>

1 **Biomineralisation performance of bacteria isolated from a**
2 **landfill in China**

3 Adharsh Rajasekar^{a,*}, Stephen Wilkinson^b, Raju Sekar^c, Jonathan Bridge^d, Eduardo-
4 Medina Roldan^e, Charles K.S.Moy^a

5 ^a Department of Civil Engineering, Xi'an Jiaotong-Liverpool University, Suzhou 215123, Jiangsu,
6 China

7 ^b Department of Civil Engineering, University of Wolverhampton, Wolverhampton WV1 1LY,
8 United Kingdom

9 ^c Department of Biological Sciences, Xi'an Jiaotong-Liverpool University, Suzhou 215123, Jiangsu,
10 China

11 ^d Department of the Natural and Built Environment, Sheffield Hallam University, Sheffield S1
12 1WB, United Kingdom

13 ^e Department of Environmental Science, Xi'an Jiaotong-Liverpool University, Suzhou 215123,
14 Jiangsu, China

15

16 *Corresponding author:

17 Adharsh Rajasekar

18 evolution.adharsh@gmail.com

19 +8618261444592

20

21

22 **Abstract**

23 We report an investigation of microbially-induced carbonate precipitation by seven
24 indigenous bacteria isolated from a landfill in China. Bacterial strains were cultured in a
25 medium supplemented with 25 mM calcium chloride and 333 mM urea. The experiments
26 were carried out at 30 °C for 7 days with agitation by a shaking table at 130 rpm. Scanning
27 Electron Microscopic (SEM) and X-ray diffraction (XRD) analyses showed variations in
28 calcium carbonate polymorphs and mineral composition induced by all bacterial strains.
29 The amount of carbonate precipitation was quantified by titration. The amount of carbonate
30 precipitated in the medium varied among isolates with the lowest being *Bacillus aerius*
31 *rawirorabr15* (LC092833) precipitating around 1.5 times more carbonate per unit volume
32 than the abiotic (blank) solution. *Pseudomonas nitroreducens szh_asesj15* (LC090854)
33 was found to be the most efficient, precipitating 3.2 times more carbonate than the abiotic
34 solution. Our results indicate that bacterial carbonate precipitation occurred through
35 ureolysis and suggest that variations in carbonate crystal polymorphs and rates of
36 precipitation were driven by strain-specific differences in urease expression and response
37 to the alkaline environment. These results and the method applied provide
38 benchmarking/screening data for assessing the bioremediation potential of indigenous
39 bacteria for containment of contaminants in landfills.

40

41 **Keywords:** Biomineralisation, Indigenous bacteria, Landfill, *Bacillus*, *Pseudomonas*,
42 SEM

43

44

45 **Introduction**

46 The potential of microbial species to stimulate precipitation of carbonates is well known in
47 various natural environments, including soils, geological formations, oceans, and saline
48 lakes (Boquet et al. 1973). This bio-mediated process is known as microbially induced
49 carbonate precipitation (MICP). The ability of these bacteria to precipitate carbonates has
50 been widely studied (Rivadeneira et al. 2006, Sanchez-Roman et al. 2007, Rivadeneira et
51 al. 2000, Rivadeneira et al. 2004, Han et al. 2013, Kang et al. 2014a). Both active and
52 passive mechanisms have been proposed to explain how bacteria mediate the precipitation
53 process (Hammes and Verstraete 2002, Silva-Castro et al. 2013). The most widely-studied
54 of these, particularly in respect of potential engineering applications, is urease hydrolysis
55 by organisms involved in the nitrogen cycle (Rivadeneira et al. 2006, Gorospe et al. 2013,
56 Achal and Pan 2014, Dhimi et al. 2014). While urease activity is common in bacteria, the
57 amount and rate of carbonate precipitation varies among species and genera and is
58 dependent on local environmental conditions (Zamarreño et al. 2009). A range of factors
59 may account for this variation: (i) rate of urea hydrolysis related to use of urea as an energy
60 source; (ii) the alkalinity of the local environment, which affects carbonate speciation and
61 CaCO_3 solubility; (iii) the affinity of the bacterial cell surfaces for Ca^{2+} ions, which can
62 create micro-scale supersaturation of Ca^{2+} in the vicinity of cells; potentially leading to (iv)
63 nucleation and crystal growth where carbonate is also sufficiently saturated.

64 In previous studies, carbonate-precipitating bacteria have been isolated from contaminated
65 and disturbed environments such as mine tailing soils (Achal and Pan 2014), caves
66 (Rusznayak et al. 2012), and highways (Kang et al. 2014a). Landfills are complex microbial

67 systems inhabited by bacteria that remediate or degrade toxic compounds (Staley et al.
68 2011). We have recently shown, for an urban landfill in China, a diverse population of
69 organisms including genera known to have biomineralisation potential (Rajasekar et al.
70 2018). Stimulating carbonate precipitation in indigenous bacteria already adapted to the
71 biochemically-harsh environmental conditions of a landfill is a potentially cost-, materials-
72 and energy-efficient alternative to geotechnical or geoenvironmental engineering
73 approaches for control of landfill leachate. Indigenous microbes could be used for
74 modification of groundwater flow, or contaminant/heavy metal immobilization by co-
75 precipitation as substitute ions for calcium or simple trapping in cemented pore spaces
76 (Ivanov and Chu 2008, Miot et al. 2009, Kang et al. 2014b, Amidi and Wang 2015). For
77 example, (Kang et al. 2014a) and (Ma et al. 2009) have used biomineralisation to trap
78 heavy metals such as cadmium. Achal et al. (2012a) utilised this technique to immobilise
79 arsenic and (Kang et al. 2015) assessed the containment of lead.

80 Access to many landfill and other controlled sites for extended investigation of
81 contamination and remediation techniques *in situ* is often logistically difficult but sampling
82 for water quality and microbiological analysis is more feasible. Thus, many more
83 biomineralisation studies have been implemented in the lab than in the field. *In situ*
84 biomineralisation to achieve geotechnical and remediation engineering objectives is still in
85 its early stages and the priority remains identification of MICP-capable organisms capable
86 of existing under specific site conditions (like landfills) and characterising their
87 biomineralisation potential (Kang et al. 2015, Kang et al. 2014a, Fujita et al. 2004, Achal
88 et al. 2012b, Kang et al. 2014b).

89 This study aims to establish a rapid laboratory protocol designed to identify, using cultures
90 isolated from landfill water samples (i) the presence of carbonate-precipitating bacteria
91 within the indigenous community; (ii) the degree of variability in bioremediation potential
92 among species; and (iii) the characteristics of MICP mechanisms demonstrated by the
93 isolates. The results offer well-constrained, benchmarking data for further studies of the
94 potential of indigenous microbes for techniques such as bioremediation or contaminants
95 containment in extreme contaminated environments such as landfills.

96 **Materials and Methods**

97 *Sampling and Storage*

98 The landfill (31°14'18.31"N 120°33'3.09"E) is located in Suzhou, Jiangsu, China. The
99 regional limestone geology is described in full in (Rajasekar et al., 2018) and the landfill
100 receives a mix of incinerator ash and raw municipal waste. Water samples were collected
101 in triplicate using a handheld peristaltic pump through sterile PVC tubing into sterile high-
102 density polyethylene (HDPE) sealable plastic bottles and stored at 4°C prior to bacterial
103 isolation. Groundwater samples were collected from boreholes on the perimeter of the
104 landfill at 4 m below surface, approximately 1.9 m below the local water table. 'Fresh'
105 leachate was collected directly from a pipe that drains the body of the landfill. 'Raw'
106 leachate was collected from an engineered leachate pond.

107 *Isolation and identification of bacterial isolates*

108 A detailed investigation of the bacterial consortia at the case study landfill site was carried
109 out using Illumina MiseqPE250 next-generation sequencing as reported previously by
110 (Rajasekar et al. 2018).

111 For this study, bacterial isolates were obtained using the following procedure. Raw and
112 fresh leachate samples with serial dilutions were spread onto nutrient agar (hopebio,
113 Qingdao, China) and incubated at 30°C for 24 hours until visible colonies were obtained.
114 The bacterial isolates were purified by repeated streaking and then transferred into nutrient
115 broth (BD, Difco™, USA). The spread plate method was also used for bacterial isolation
116 from an undiluted 100µl groundwater aliquot and the isolates were purified by repeated
117 streaking. The cells were harvested and pellets directly transferred to the bead columns for
118 DNA extraction. The genomic DNA was extracted using PowerSoil® DNA isolation kit
119 (MO BIO, USA) following the manufacturer's instructions. The 16S rRNA genes were
120 amplified using PCR with 10 mM concentration of 27F and 1492R primers (Muyzer et al.
121 1993). A final volume of 50 µL was used in the PCR assay, which contains 10X PCR buffer
122 (5 µL), 10 mmol/L dNTPs (1 µL), 25 mmol/L MgCl₂ (4 µL), forward and reverse primers
123 10mM each (2µL), Taq polymerase (2 U), DNA template (1 µL), and 37 µL of double-
124 distilled water. The PCR cycling conditions were as follows: initial denaturation at 94 °C
125 for 4 minutes followed by 30 cycles of denaturation at 94 °C for 1 minute, annealing at 55
126 °C for 35 seconds, extension for 1 minute at 72 °C; after 30 cycles final extension at 72 °C
127 for 10 minutes. The PCR products were verified by agarose gel (1.5% wt/v) electrophoresis
128 and purified using a PCR purification kit (Axygen®, CA, USA). The purified PCR products
129 were sequenced at a sequencing facility (Sangon Biotech Co Ltd) in Shanghai, China using
130 27F primer. The partial sequences were compared using BLAST queuing system (Altschul
131 et al. 1990) to identify their closest relatives and tentative phylogenetic positions. The
132 sequences were later submitted to DNA Data Bank of Japan (DDBJ) for acquisition of

133 unique accession numbers for the sequences (LC090023, LC092830-33, and LC090854-
134 55).

135 *Urease activity assay*

136 The isolates were tested for urease activity on urea agar media using the method described
137 by (Hammes et al. 2003). All the isolates tested positive for urease enzyme. This was
138 confirmed after 5 days of incubation at 28°C.

139 *Biom mineralisation assay*

140 Biom mineralisation media consisted of 25 mM calcium chloride solution (purity $\geq 98\%$), 333
141 mM of urea solution (purity $\geq 97\%$) and 0.8 g of nutrient broth (BD, Difco™, USA) per
142 150 ml consistent with published methods used in previous MICP studies (Kang et al.
143 2014a, Muynck et al. 2010b, Helmi et al. 2016, Muynck et al. 2010a, Achal and Pan 2014).
144 The initial pH was 9.1 and adjust to pH 7.5 with HCl. Calcium chloride solution was
145 autoclaved and filter-sterilized to avoid any contamination before mixing. Urea solution
146 was only filter-sterilized to avoid denaturing of the urea at high temperatures. Two mL of
147 the bacterial culture (grown overnight in nutrient broth at 30 °C for 24 hours) were added
148 to 150 mL of the biom mineralisation media and incubated in a rotary shaker at 120 rpm for
149 7 days at 30 °C. Sterile biom mineralisation media without bacterial isolates was used as a
150 blank control. The pH of the bacterial and abiotic control solutions were recorded using a
151 Suntex TS1 pH meter once every 24 hours. The pH was checked under a laminar hood to
152 avoid any potential contamination. After 7 days of incubation, the solution was vacuum
153 filtered through a sterile 0.6 μm Whatman® membrane filter (Whatman®, USA). Each filter
154 paper was placed in a separate sterile Petri dish and air dried at 37°C for 24 hours for
155 subsequent analyses. All incubations were carried out in triplicate.

156 ***Scanning Electron Microscopy (SEM)***

157 Fragments of residue from each filter paper were transferred onto double-sided carbon tape
158 affixed to standard 5 mm electron microscope stubs for imaging using an Hitachi TM3000
159 scanning electron microscope. Five mm stubs were used to allow easy transportation and
160 storage of samples for future observation and an adaptor was used to allow the stubs to be
161 inserted on top of the Hitachi TM3000 stage. The samples were imaged uncoated, under
162 relatively low vacuum conditions. Images were taken at magnifications between 400× and
163 1500× to allow the identification of crystals formed due to biomineralisation. Due to the
164 low magnification used, no charging errors were recorded during imaging.

165 ***X-ray powder diffraction (XRD) analysis***

166 A powder sample was created by scraping residue from the filter papers using a sterile razor
167 blade directly onto the sample holder of the X-ray diffractometer (Advanced D8, Bruker,
168 Germany). The upper surface was then carefully flattened using a glass slide. The sample
169 holder was rotated during measurement to ensure good sampling of the crystal lattices
170 within the powder sample.

171 ***Carbonate titration analysis***

172 The total carbonate present in the residue on each filter was quantified using titration
173 following the method of (Maulood et al. 2012). The amount of residue (grams) that's
174 deposited on the filter paper after filtration influences the value of carbonate precipitation
175 since all the residue that's deposited on the paper is used for titration. The residue is
176 weighed before the titration to calculate the amount of carbonate precipitated during the
177 process.

178 **Results**

179 ***Identification of bacterial isolates by 16S rRNA gene sequencing***

180 Five strains isolated from landfill leachate belonged to members of genus *Bacillus*. Among
181 these, two were isolated from raw leachate and three from fresh leachate samples (Table
182 1). The bacteria isolated from landfill groundwater belonged to the genera *Pseudomonas*
183 and *Sphingopyxis*. Two indigenous bacterial strains isolated from the landfill groundwater
184 were identified as *Pseudomonas nitroreducens* szh_asesj15 (LC090854) and *Sphingopyxis*
185 sp. szh_adharsh (LC090855) by 16S rRNA gene sequencing (Table 1). *Pseudomonas*
186 belongs to γ -Proteobacteria and has commonly been found in landfills (Kalwasinska and
187 Burkowska 2013). *Sphingopyxis* belongs to α -Proteobacteria, and members of this genus
188 are extremely resistant towards soil contamination such as that from high heavy metal
189 concentrations (Choi et al. 2010).

190 ***pH variation with time during biomineralisation assay***

191 Figure 1 A shows the change in pH as a function of time during the biomineralisation
192 assays. Landfill leachate isolates (Fig. 1A) experienced a lag phase during the first 24 hours
193 in which pH remained steady, while in experiments with isolates from groundwater the pH
194 started to increase immediately (Fig. 1B). Steady rise in pH was observed in all assays from
195 24 h through 144 h, with the highest value obtained by *Sphingopyxis* isolated from landfill
196 groundwater (mean pH 10 ± 0.1). The pH of medium with *Bacillus licheniformis*
197 SZH2015_A was found to be decreasing after 120 hours, which was not observed in any
198 of the other bacterial isolates (Fig. 1 A). In the abiotic control, pH increased steadily from
199 pH 7.5 to pH 8.5 (± 0.033) from 0-144 h (Figure 1 B).

200 ***SEM analysis***

201 Figures 2 and 3 illustrate the range of calcium carbonate crystal morphologies observed in

202 SEM. Spherical crystals were ubiquitous in all bacterial experiments but rare or absent in
203 abiotic controls, where rhombohedral crystals dominated. Morphological distinction was
204 observed in certain crystals from bacterial isolates (Fig. 3 A & B). In some cases, evidence
205 was observed of direct bacteria-crystal contacts. Fig. 3B shows elongate pits on the surface
206 of a crystal. Fig. 2E shows the growth of micro crystals on the surface of a calcite crystal.
207 Two different types of crystal fusion were observed in Fig. 2A and Fig. 3A which has the
208 potential of resulting in the formation of one larger crystal.

209 *XRD analysis*

210 XRD spectra indicated the primary component of all the precipitates was Calcite, although
211 Vaterite was detected in some cases as well.

212 *Carbonate quantification*

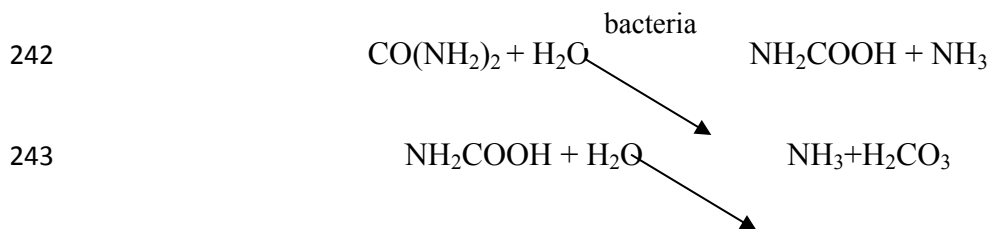
213 Comparison between the urease activities of the isolates was determined using carbonate
214 titration. The isolate with the highest pH value was not found to have the highest carbonate
215 precipitation (Fig. 6). *Pseudomonas nitroreducens* szh_asesj15 was observed to have the
216 highest carbonate precipitation (0.88 ± 0.2), while *Bacillus pumilus* szhxjlu2015 was
217 observed to have the lowest carbonate precipitation (0.41 ± 0.3). The blank was observed
218 to have the lowest carbonate precipitation when compared with bacterial isolates which is
219 expected since it has no urease activity.

220 **Discussion**

221 *Analysis of pH in bacterial and blank solutions*

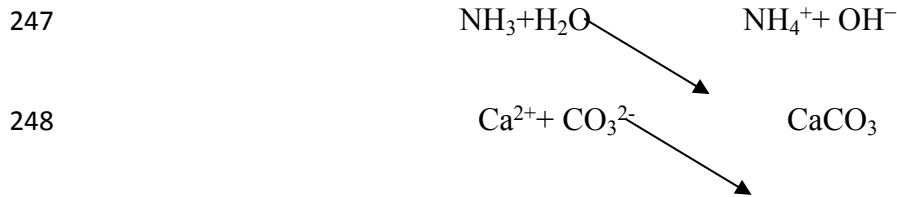
222 The maximum pH measurements for all of the bacterial isolates exceeded that of the blank
223 (Fig. 1 A&B). This was expected since the blank did not have the urease enzyme. The pH
224 surge within 24 hours of the experiment observed in the leachate isolates was quite

225 different when compared with the groundwater isolates. Even among the leachate bacteria,
 226 pH variations could be observed. This indicated that each bacterium undergoes different
 227 rates of ureolysis for carbonate precipitation. During the first 24 hours of incubation, the
 228 pH of the *Bacillus pumilus szhxjlu2015* and *Bacillus aerius rawirorabr15* decreased from
 229 their initial pH values (Fig. 1 A). This was probably due to the different adaptation time
 230 of the bacteria to the environment for urea hydrolysis (Lian et al. 2006). Bacteria such as
 231 *Bacillus subtilis* have been shown to pump out protons through their cell walls during
 232 respiration (Mera et al. 1992). These protons will presumably occupy the negatively
 233 charged cell surface sites and lower the pH of the local environment. This early reduction
 234 in pH has also been observed by (Rivadeneira et al. 2006, Sanchez-Roman et al. 2007). In
 235 comparison to Figs. 1 A and B shows an increase in pH from 7.5 to ~8.4 for the
 236 groundwater bacteria during the first 24 hours following inoculation into biomineralisation
 237 medium. It has been reported that certain ureolytic bacteria begin the process of urea
 238 hydrolysis within 24 hours for carbonate precipitation (Achal and Pan 2014). For the
 239 groundwater bacteria, the pH increased almost linearly over 144 hours presumably because
 240 of the consistent enzymatic hydrolysis of urea and higher CO_3^{2-} precipitation and upon
 241 depletion of the dissolved urea results in an reduction in pH (Stocks-Fischer et al. 1999).



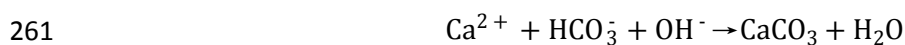
244 These products equilibrate in water to form bicarbonate, 1 mole of ammonium and
 245 hydroxide ions which give rise to pH increase





249 A similar trend was also observed with the bacteria isolated from leachate after 48 hours
 250 (Fig. 1 A). All the leachate bacteria are in their linear progressive state (consistent increase
 251 in pH) indicated by the bacterial enzymatic hydrolysis of urea leading to an increased
 252 production in $[\text{OH}^-]$ ions which contributes to the pH increase.

253 At this pH, a substantial amount of carbonate is present in the solution (the pKa of HCO_3^{2-}
 254 $-\text{CO}_3^{2-}$ is approximately one order of magnitude higher), which in turn, in the presence of
 255 calcium ions, can lead to a supersaturation of carbonate in the solution, thereby promoting
 256 the precipitation of calcium carbonate. The forward reaction is catalysed by microbes, thus
 257 allowing the generation of a higher peak pH in the bacterial solutions in comparison to the
 258 control (Fujita et al. 2008). The reduction in pH can be explained using two chemical
 259 reactions, the precipitation of calcium carbonate and the conversion of ammonium to
 260 ammonia:



263

264 The pH values from this study can be explained using the theory proposed by (Sanchez-
 265 Roman et al. 2007) for ureolysis. They reported that the activity of urease is optimum at a
 266 pH of 8.5, leading to superior carbonate precipitation (Gorospe et al. 2013, Stabnikov et al.
 267 2013, Chu et al. 2014). They indicated that the metabolic activity of the bacteria is
 268 extremely important and it varies from one bacteria to another. Each bacteria supplies the

269 ions necessary for the formation of the minerals, namely NH_4^+ and CO_3^{2-} for carbonates.
270 Moreover, the appropriate microenvironment is created for precipitation, i.e. increased pH
271 and/or ionic concentration. This increased pH environment was also observed in our study
272 for all the bacteria. This demonstrates that bacteria are not simply heterogeneous nuclei for
273 precipitation but are also active mediators in the process.

274 Furthermore, the bacterial degradation of peptones and yeast extract takes place, supplying
275 NH_4^+ leading to an increase of pH, as observed in our experiments. The metabolic activity
276 occurring in the media, together with the concentration of ions in the cellular envelopes,
277 will drive local oversaturation of such ions, leading to carbonate precipitation. The pH
278 change in the abiotic solution was also observed by (Ferris et al. 2003, Gorospe et al. 2013,
279 Achal and Pan 2014) and it is attributed to the very slow hydrolysis of urea which is
280 speculated to be 10^{14} slower than a biotic hydrolysis of urea.

281 The presence of bacteria can induce the precipitation of minerals in microenvironments by
282 the combination of two mechanisms; (1) modifying the conditions of their surrounding
283 environments through ureolysis and/or the concentration of ions in the bacterial cell
284 envelope (Li et al. 2013); and (2) cell walls acting as nucleation sites for the growth of the
285 carbonate crystals (Li et al. 2011).

286 *Morphology of crystals in bacterial and control solutions*

287 Previous SEM studies of carbonates formed due to MICP have identified that spherical
288 crystal forms are commonly observed in samples containing bacteria in comparison to the
289 normal rhombohedral crystal form (trigonal system) in non-bacterial samples (Stocks-
290 Fischer et al. 1999, Rivadeneyra et al. 2004, Lian et al. 2006, Jimenez-Lopez et al. 2007,
291 Sánchez-Román et al. 2011). It has been suggested that spherical crystals are a result of the

292 higher rate of crystal formation which is occurring due to the action of the ureolytic bacteria
293 (Stocks-Fischer et al. 1999). The SEM images obtained for the seven bacterial isolates also
294 showed this spherical crystal morphology (Fig. 2A, B, C, D, E; Fig 3 A and B). Very similar
295 observations have been made for the well-studied ureolytic bacteria, *Bacillus megaterium*
296 (Lian et al. 2006). Further to this, the full range of observations displayed in Fig. 2 and 3
297 indicate that the bacterial strains influence both the crystal morphology and growth patterns.
298 Similar observations have been individually reported across a range of studies for other
299 biomineralising organisms (Rivadeneira et al. 2000, Rivadeneira et al. 2004, Lian et al.
300 2006, Jimenez-Lopez et al. 2007). The main reason for the changes in morphology is
301 probably due to the differences in ureolysis rates influenced by the bacterial density
302 (Rodriguez-Navarro et al. 2012) and the saturation index of the solution (Bosak and
303 Newman 2005, Sanchez-Roman et al. 2007, Mitchell and Ferris 2006).

304 Fused spherical crystals were observed in *Bacillus licheniformis* SZH2015_A (Fig. 2A) &
305 *Bacillus aerius* rawirorabr15 (Fig. 2E) samples, where the spherical crystals have grown
306 together and become interlocked. Xu et al. (2015) suggested that calcium sources are highly
307 influential in the clumping or fusing of crystals. This type of crystal formation is highly
308 desirable for soil applications, as it can generate very low permeability zones within a soil
309 allowing pore necks to become sealed. At a larger scale, clumping of large numbers of
310 calcite crystals is produced by *Bacillus licheniformis* adseedstjo15 (Fig. 2E). Clumping of
311 crystals occurs when the expansion of crystals displaces and entrains smaller growing
312 crystals. This leads to the formation of an interlocking framework that enables bacteria to
313 slowly establish contact with nearby crystals surfaces and develop colonies on them (Wang
314 et al. 2013). The structure which forms is not a completely fused crystal, although it is

315 likely to contain fused crystals. Such structures will have the effect of reducing
316 permeability, but not to the extent of a fully interlocking crystalline structure.

317 Bacterial imprints were also identified on the surface of calcite crystals for *Sphingopyxis*
318 sp. szh_adharsh (Fig. 3B). These results suggested that the bacteria might serve as
319 nucleation sites for calcite precipitation, which is in agreement with observations with other
320 carbonate precipitating bacteria (Lian et al. 2006, Li et al. 2011). The bacterial cell surface
321 could induce mineral deposition by providing nucleation sites due to ion composition on
322 its surface (Lian et al. 2006). Ion composition is referred to as the negatively charged
323 functional groups that are present on the bacterial cell walls which attract Ca^{2+} to induce a
324 local supersaturation so that calcite nucleation takes place on the cell surfaces. No spherical
325 calcite forms were observed in the blank sample (Fig. 3F).

326 ***X-Ray diffraction (XRD) analysis***

327 XRD analysis was used to measure the composition, structure and microstructure of the
328 crystal compounds. Calcium carbonate crystals were precipitated by all the bacterial
329 isolates in this study (Fig. 4 & 5). Calcite and vaterite were produced in all samples. The
330 results, especially from the use of calcium chloride, concur with the previous reports in
331 which calcite and vaterite were produced (Gorospe et al. 2013). Zamarreño et al. (2009)
332 reported that precipitation of calcite and vaterite were also influenced by the bacteria and
333 the carbonate precipitation media. To our knowledge, our study indicates that bacteria
334 rather than calcium chloride caused differences in the morphology of calcium carbonate
335 polymorphs (Fig. 4 & 5). This is a very important finding because it suggests that each
336 bacteria precipitate calcium carbonate polymorphs in a slightly different way in the same
337 media.

338

339 ***Quantification of Carbonate***

340 Titration was performed to calculate and compare the efficiency of carbonate precipitation
341 by each bacterium. The final quantities of precipitated calcium carbonate were confirmed
342 through titration with 0.5 M HCl. Previous studies have shown that urease production
343 increases the pH resulting in a superior carbonate precipitation (Achal and Pan 2014).
344 Observations in our study differ from this conclusion, as the pH of *Bacillus* sp. xjlu_herc15
345 reached a higher pH than *Pseudomonas nitroreducens* szh_asesj15. However, *Bacillus* sp.
346 xjlu_herc15 precipitated 0.8 grams of carbonate compared to *Pseudomonas nitroreducens*
347 szh_asesj15 which precipitated 0.9 grams (Fig. 6). Although *Bacillus* sp. xjlu_herc15 took
348 time to adapt to the environment in comparison to the other bacteria, it still managed to
349 precipitate a superior quantity of carbonate compared to the other five bacteria. Given that
350 pH rise is correlated with urease activity, *Bacillus* sp. xjlu_herc15 has shown to have
351 superior enzyme activity compared to other bacteria from the landfill between 48 to 144
352 hours. For all of the bacterial samples, the amount of precipitation was higher than that of
353 the abiotic (blank) solution. The variation in effectiveness ranged from 1.53 to 3.2 times
354 more CaCO₃ precipitation per 150 ml retained on the filter paper compared to the abiotic
355 (blank) sample (Fig. 6). No carbonate precipitation was found in the abiotic samples
356 reported by Sanchez-Roman et al. 2007, Achal and Pan 2014 but recent studies conducted
357 by Zamarreño et al. 2009a, Okyay and Rodrigues 2015 reported carbonate precipitation
358 under abiotic conditions. Okyay and Rodrigues (2015) suggested that the interaction of
359 CO₂ with the abiotic media results in the precipitation of carbonate.

360 **Conclusions**

361 Studies based on MICP have shown that the composition of the culture medium and pH
362 can change the type and amount of calcium carbonate precipitated. This study focuses
363 mainly on the biomineralisation potential of indigenous bacteria from a landfill and its
364 surroundings. Hence, we provide strong evidence of such possibility and present data
365 showing the precipitation performance of a range of newly identified bacterial strains.
366 Analysis of the microbially induced calcium carbonate produced was achieved using a
367 combination of carbonate titration, SEM and XRD methods. Each bacteria, irrelevant of
368 their environment, influenced the morphology and amount of calcium carbonate
369 precipitation. Bacterial strain was identified as more important than pH in terms of the
370 amount of carbonate being precipitated by the bacteria. Even though, urease activity does
371 promote carbonate precipitation, it does not appear to be the sole determining factor of the
372 amount of carbonate that will be precipitated. This approach makes it ideal for
373 biostimulation of these bacteria in the landfill for environmental remediation purposes.
374 Therefore, the authors hope that the findings from this study will potentially lead to an
375 optimistic implication for the design of future engineering applications involving
376 microbially induced calcite precipitation, such as sand consolidation, soil improvement,
377 and bioremediation.

378 **Acknowledgements**

379 This work was supported by grant no. PGRS-12-02-06 and RDF-13-01-06 awarded by
380 XJTLU.

381 **Conflict of interest**

382 No conflict of interest declared.

383

384 **References**

- 385 ACHAL, V. & PAN, X. 2014. Influence of calcium sources on microbially induced
386 calcium carbonate precipitation by *Bacillus* sp. CR2. *Appl Biochem Biotechnol*, 173,
387 307-317.
- 388 ACHAL, V., PAN, X., FU, Q. & ZHANG, D. 2012a. Biomineralization based remediation
389 of As(III) contaminated soil by *Sporosarcina ginsengisoli*. *J Haz Mat*, 201-202,
390 178-184.
- 391 ACHAL, V., PAN, X. & ZHANG, D. 2012b. Bioremediation of strontium (Sr)
392 contaminated aquifer quartz sand based on carbonate precipitation induced by Sr
393 resistant *Halomonas* sp. *Chemosphere*, 89, 764-768.
- 394 AMIDI, S. & WANG, J. 2015. Surface treatment of concrete bricks using calcium
395 carbonate precipitation. *Constr Buil Mat*, 80, 273-278.
- 396 BOQUET, A. BORONAT & A. RAMOS-CORMENZANA 1973. Production of Calcite
397 (Calcium Carbonate) crystals by soil bacteria is a general phenomenon. *Nature*, 246,
398 527-529.
- 399 BOSAK, T. & NEWMAN, D. K. 2005. Microbial kinetic controls on calcite morphology
400 in supersaturated solutions. *J Sedimen res*, 75, 190-199.
- 401 CHOI, J. H., KIM, M. S., JUNG, M. J., ROH, S. W., SHIN, K. S. & BAE, J. W. 2010.
402 *Sphingopyxis soli* sp. nov., isolated from landfill soil. *Int J Sys Evol Microbiol*, 60,
403 1682-1686.
- 404 CHU, J., IVANOV, V., NAEIMI, M., STABNIKOV, V. & LIU, H.-L. 2014. Optimization
405 of calcium-based bioclogging and biocementation of sand. *Acta Geotechnica*, 9,
406 277-285.
- 407 DHAMI, N. K., REDDY, M. S. & MUKHERJEE, A. 2014. Synergistic Role of Bacterial
408 Urease and Carbonic Anhydrase in Carbonate Mineralization. *Appl Biochem
409 Biotechnol*, 172, 2552-2561.
- 410 FERRIS, F. G., V. PHOENIX, FUJITA, Y. & SMITH, R. W. 2003. Kinetics of calcite
411 precipitation induced by ureolytic bacteria at 10 to 20°C in artificial groundwater.
412 *Geochimica et Cosmochimica Acta*, 67, 1701-1722.

- 413 FUJITA, Y., REDDEN, G. D., INGRAM, J. C., CORTEZ, M. M., FERRIS, F. G. &
414 SMITH, R. W. 2004. Strontium incorporation into calcite generated by bacterial
415 ureolysis. *Geochim Cosmochim Acta*, 68, 3261-3270.
- 416 FUJITA, Y., TAYLOR, J. L., GRESHAM, T. L. T., DELWICHE, M. E., COLWELL, F.
417 S., MCLING, T. L., PETZKE, L. M. & SMITH, R. W. 2008. Stimulation Of
418 Microbial Urea Hydrolysis In Groundwater To Enhance Calcite Precipitation.
419 *Environ sci technol*, 42, 3025-3032.
- 420 GOROSPE, C. M., HAN, S.-H., KIM, S.-G., PARK, J.-Y., KANG, C.-H., JEONG, J.-H.
421 & SO, J.-S. 2013. Effects of Different Calcium Salts on Calcium Carbonate Crystal
422 Formation by *Sporosarcina pasteurii* KCTC 3558. *Biotechnol Biopro Eng*, 18, 903-
423 908.
- 424 HAMMES, F., BOON, N., VILLIERS, J. D., VERSTRAETE, W. & SICILIANO, S. D.
425 2003. Strain-Specific Ureolytic Microbial Calcium Carbonate Precipitation. *Appl*
426 *Environ Microbiol*, 69, 4901-4909.
- 427 HAMMES, F. & VERSTRAETE, W. 2002. Key roles of pH and calcium metabolism in
428 microbial carbonate precipitation. *Re/Views in Environ Sci BioTechnol*, 1, 3-7.
- 429 HAN, Z., YAN, H., ZHOU, S., ZHAO, H., ZHANG, Y., ZHANG, N., YAO, C., ZHAO,
430 L. & HAN, C. 2013. Precipitation of calcite induced by *Synechocystis* sp. PCC6803.
431 *W J Microbiol Biotechnol*, 29, 1801-1811.
- 432 HELMI, F. M., ELMITWALLI, H. R., ELNAGDY, S. M. & EL-HAGRASSY, A. F. 2016.
433 Calcium carbonate precipitation induced by ureolytic bacteria *Bacillus*
434 *licheniformis*. *Ecol Eng*, 90, 367-371.
- 435 IVANOV, V. & CHU, J. 2008. Applications of microorganisms to geotechnical
436 engineering for bioclogging and biocementation of soil in situ. *Reviews in Environ*
437 *Sci Bio/Technol*, 7, 139-153.
- 438 JIMENEZ-LOPEZ, C., JROUNDI, F., RODRÍGUEZ-GALLEGO, M., ARIAS, J. M. &
439 GONZALEZ-MUÑOZ, M. T. 2007. Biomineralization induced by Myxobacteria.
440 *Communicating Curr Res Educational Topics and Trends in Appl Microbiol*, 143-
441 154.

- 442 KALWASINSKA, A. & BURKOWSKA, A. 2013. Municipal landfill sites as sources of
443 microorganisms potentially pathogenic to humans. *Environ Sci Processes &*
444 *Impacts*, 15, 1078-1086.
- 445 KANG, C.-H., HAN, S.-H., SHIN, Y., OH, S. J. & SO, J.-S. 2014a. Bioremediation of Cd
446 by Microbially Induced Calcite Precipitation. *Appl Biochem Biotechnol*, 172, 2907-
447 2915.
- 448 KANG, C.-H., OH, S. J., SHIN, Y., HAN, S.-H., NAM, I.-H. & SO, J.-S. 2015.
449 Bioremediation of lead by ureolytic bacteria isolated from soil at abandoned metal
450 mines in South Korea. *Ecol Eng*, 74, 402-407.
- 451 KANG, C. H., CHOI, J. H., NOH, J., KWAK, D. Y., HAN, S. H. & SO, J. S. 2014b.
452 Microbially induced calcite precipitation-based sequestration of strontium by
453 *Sporosarcina pasteurii* WJ-2. *Appl Biochem Biotechnol*, 174, 2482-2491.
- 454 LI, W., CHEN, W.-S., ZHOU, P.-P., ZHU, S.-L. & YU, L.-J. 2013. Influence of initial
455 calcium ion concentration on the precipitation and crystal morphology of calcium
456 carbonate induced by bacterial carbonic anhydrase. *Chem Eng J*, 218, 65-72.
- 457 LI, W., LIU, L.-P., ZHOU, P.-P., CAO, L., YU, L.-J. & JIANG, S.-Y. 2011. Calcite
458 precipitation induced by bacteria and bacterially produced carbonic anhydrase.
459 *Curr sci*, 100, 502-508.
- 460 LIAN, B., HU, Q., CHEN, J., JI, J. & TENG, H. H. 2006. Carbonate biomineralization
461 induced by soil bacterium *Bacillus megaterium*. *Geochim Cosmochim Acta*, 70,
462 5522-5535.
- 463 MA, Y., LIN, C., JIANG, Y., LU, W., SI, C. & LIU, Y. 2009. Competitive removal of
464 water-borne copper, zinc and cadmium by a CaCO₃-dominated red mud. *J Haz Mat*,
465 172, 1288-1296.
- 466 MAULOOD, P. M., ESMAIL, A. O., DOHUKI, M. S. S. & DARWESH, D. A. 2012.
467 Comparison between Calcimetric and Titrimetric Methods for Calcium Carbonate
468 Determination. *Open J Soil Sci*, 2, 263-268.
- 469 MERA, M. U., KEMPER, M., DOYLE, R. & BEVERIDGE, T. J. 1992. The membrane-
470 induced proton motive force influences the metal-binding ability of *Bacillus subtilis*
471 cell walls. *Appl Environ Microbiol*, 58, 3837-3844.

- 472 MIOT, J., BENZERARA, K., OBST, M., KAPPLER, A., HEGLER, F., SCHADLER, S.,
473 BOUCHEZ, C., GUYOT, F. & MORIN, G. 2009. Extracellular iron
474 biomineralization by photoautotrophic iron-oxidizing bacteria. *Appl Environ*
475 *Microbiol*, 75, 5586-5591.
- 476 MITCHELL, A. C. & FERRIS, F. G. 2006. The Influence of *Bacillus pasteurii* on the
477 Nucleation and Growth of Calcium Carbonate. *Geomicrobiol J*, 23, 213-226.
- 478 MUYNCK, W. D., BELIE, N. D. & VERSTRAETE, W. 2010a. Microbial carbonate
479 precipitation in construction materials: A review. *Ecol Eng*, 36, 118-136.
- 480 MUYNCK, W. D., VERBEKEN, K., BELIE, N. D. & VERSTRAETE, W. 2010b.
481 Influence of urea and calcium dosage on the effectiveness of bacterially induced
482 carbonate precipitation on limestone. *Ecol Eng*, 36, 99-111.
- 483 MUYZER, G., WAAL, E. C. D. & UITIERLINDEN, A. G. 1993. Profiling of Complex
484 Microbial Populations by Denaturing Gradient Gel Electrophoresis Analysis of
485 Polymerase Chain Reaction-Amplified Genes Coding for 16S rRNA. *Appl Environ*
486 *Microbiol*, 59, 695-700.
- 487 OKYAY, T. O. & RODRIGUES, D. F. 2015. Biotic and abiotic effects on CO₂
488 sequestration during microbially-induced calcium carbonate precipitation. *FEMS*
489 *Microbiol Ecol*, 91, 1-13.
- 490 RAJASEKAR, A., RAJU, S., MEDINA-ROLDAN, E., BRIDGE, J., K.S.MOY, C. &
491 WILKINSON, S. 2018. Next-generation sequencing showing potential leachate
492 influence on bacterial communities around a landfill in China. *Can J Microbiol*.
- 493 RIVADENEYRA, M. A., DELGADO, G., SORIANO, M., RAMOS-CORMENZANA, A.
494 & DELGADO, R. 2000. Precipitation of carbonates by *Nesterenkonia halobia* in
495 liquid media. *Chemosphere*, 41, 617-624.
- 496 RIVADENEYRA, M. A., MARTÍN-ALGARRA, A., SÁNCHEZ-NAVAS, A. &
497 MARTÍN-RAMOS, D. 2006. Carbonate and Phosphate Precipitation by
498 *Chromohalobacter marismortui*. *Geomicrobiol J*, 23, 1-13.
- 499 RIVADENEYRA, M. A., PARRAGA, J., DELGADO, R., RAMOS-CORMENZANA, A.
500 & DELGADO, G. 2004. Biomineralization of carbonates by *Halobacillus trueperi*
501 in solid and liquid media with different salinities. *FEMS Microbiol Ecol*, 48, 39-
502 46.

- 503 RUSZNYAK, A., AKOB, D. M., NIETZSCHE, S., EUSTERHUES, K., TOTSCHKE, K.
504 U., NEU, T. R., FROSCH, T., POPP, J., KEINER, R., GELETNEKY, J.,
505 KATZSCHMANN, L., SCHULZE, E. D. & KUSEL, K. 2012. Calcite
506 biomineralization by bacterial isolates from the recently discovered pristine karstic
507 herrenberg cave. *Appl Environ Microbiol*, 78, 1157-1167.
- 508 SANCHEZ-ROMAN, M., RIVADENEYRA, M. A., VASCONCELOS, C. &
509 MCKENZIE, J. A. 2007. Biomineralization of carbonate and phosphate by
510 moderately halophilic bacteria. *FEMS Microbiol Ecol*, 61, 273-284.
- 511 SÁNCHEZ-ROMÁN, M., ROMANEK, C. S., FERNÁNDEZ-REMOLAR, D. C.,
512 SÁNCHEZ-NAVAS, A., MCKENZIE, J. A., PIBERNAT, R. A. &
513 VASCONCELOS, C. 2011. Aerobic biomineralization of Mg-rich carbonates:
514 Implications for natural environments. *Chem Geol*, 281, 143-150.
- 515 SILVA-CASTRO, G. A., UAD, I., RIVADENEYRA, A., VILCHEZ, J. I., MARTIN-
516 RAMOS, D., GONZÁLEZ-LÓPEZ, J. & RIVADENEYRA, M. A. 2013.
517 Carbonate Precipitation of Bacterial Strains Isolated from Sediments and Seawater:
518 Formation Mechanisms. *Geomicrobiol J*, 30, 840-850.
- 519 STABNIKOV, V., JIAN, C., IVANOV, V. & LI, Y. 2013. Halotolerant, alkaliphilic
520 urease-producing bacteria from different climate zones and their application for
521 biocementation of sand. *W J Microbiol Biotechnol*, 29, 1453-1460.
- 522 STALEY, B. F., SAIKALY, P. E., DE LOS REYES, F. L., 3RD & BARLAZ, M. A. 2011.
523 Critical evaluation of solid waste sample processing for DNA-based microbial
524 community analysis. *Biodegradation*, 22, 189-204.
- 525 STOCKS-FISCHER, S., GALINAT, J. K. & BANG, S. S. 1999. Microbiological
526 precipitation of CaCO₃. *Soil Biol Biochem*, 31, 1563-1571.
- 527 WANG, Y.-Y., YAO, Q.-Z., ZHOU, G.-T. & FU, S.-Q. 2013. Formation of elongated
528 calcite mesocrystals and implication for biomineralization. *Chem Geol*, 360-361,
529 126-133.
- 530 XU, J., DU, Y., JIANG, Z. & SHE, A. 2015. Effects of Calcium Source on Biochemical
531 Properties of Microbial CaCO₃ Precipitation. *Front Microbiol*, 6, 1-7.

532 ZAMARREÑO, D. V., INKPEN, R. & MAY, E. 2009. Carbonate crystals precipitated by
533 freshwater bacteria and their use as a limestone consolidant. *Appl Environ*
534 *Microbiol*, 75, 5981-5990.

535

536

537

538

539

540

541

542

543

544

545

546

547

548

549

550

551

552

553

554

555

556 **Figure Legends**

557 **Fig 1. (A)** Changes in the pH of the biomineralisation medium (along with a blank) during
558 the growth of the bacteria isolated from groundwater. **(B)** Changes in the pH of the
559 biomineralisation medium (along with a blank) during the growth of the bacteria isolated
560 from leachate. Data points are means of experiments performed in triplicate and error bars
561 represent the variations obtained during the pH readings.

562 **Fig 2.** Spherical calcite crystals found in solutions containing **(A)** *Bacillus licheniformis*
563 SZH2015_A, (1) fusing of two calcite crystals. **(B)** *Bacillus pumilus* szhxjlu2015, (2)
564 fibrous patterns on the surface of a spherical calcite crystal. **(C)** *Bacillus* sp. xjlu_here15,
565 (3) very small calcite crystals (<30µm) on the surface of a single calcite crystal. **(D)**
566 *Bacillus licheniformis* adseedstjo15, (4) single spherical calcite crystal connected with
567 non-spherical calcite crystals. **(E)** *Bacillus aerius* rawirorabr15, (5) small calcite crystals
568 (50-75µm) fused together on the top of a calcite crystals, (6) minor cracks observed on the
569 surface of a calcite crystals and non-spherical calcite crystal with platy overlapping layers
570 on the surface of the calcite crystal observed in. **(F)** abiotic solution showing rhombohedral
571 crystal forms.

572 **Fig 3.** Scanning electron micrographs showing mineral precipitates formed in the presence
573 of *Pseudomonas nitroreducens* szh_asesj15 **(A)** Radiating growth structures in the crystal
574 (1) and internal fusing lines on a spherical calcite crystal (2). **(B)** Arrows indicate bacterial
575 imprints on the surface of calcite crystals formed in the presence of *Sphingopyxis* sp.
576 szh_adharsh.

577 **Fig 4.** XRD spectra indicating multiple calcite and vaterite peaks in all five bacterial
578 isolates and the blank. **(A)** *Bacillus licheniformis* SZH2015_A; **(B)** *Bacillus pumilus*

579 szhxjlu2015; **(C)** *Bacillus sp.* xjlu_herc15; **(D)** *Bacillus licheniformis* adseedstjo15; **(E)**
580 *Bacillus aerius* rawirorabr15 and **(F)** abiotic solution. (Ca= Calcite; V= Vaterite).

581 **Fig 5.** XRD spectra showing multiple calcites and a single vaterite peak for the bacterial
582 samples. A = *Pseudomonas nitroreducens* szh_asesj15; B = *Sphingopyxis* sp. szh_adharsh.
583 Ca=Calcite and V=Vaterite respectively.

584 **Fig 6.** Calcium carbonate precipitation with error bars for individual bacterial solutions **(A)**
585 *Bacillus sp.* xjlu_herc15 **(B)** *Bacillus licheniformis* adseedstjo15 **(C)** *Bacillus licheniformis*
586 SZH2015_A **(D)** *Bacillus aerius* rawirorabr15 **(E)** *Bacillus pumilus* szhxjlu2015 **(F)**
587 *Pseudomonas nitroreducens* szh_asesj15 **(G)** *Sphingopyxis* sp. szh_adharsh and **(H)**
588 abiotic solution.

589

Table 1. Details of the 16S rRNA gene sequences retrieved from bacteria isolated from Landfill raw and fresh leachates and groundwater, respectively.

Source	Accession number	Name of bacteria	Percentage identity	Closest relative in Genbank with accession number
Landfill leachate (raw)	LC090023	<i>Bacillus licheniformis</i> SZH2015_A	98%	<i>Bacillus licheniformis</i> LRF2X (KX364925)
Landfill leachate (raw)	LC092830	<i>Bacillus pumilus</i> szhxjlu2015	98%	<i>Bacillus pumilus</i> Bp02 (KJ438145)
Landfill leachate (fresh)	LC092831	<i>Bacillus</i> sp. xjlu_herc15	97%	Uncultured <i>Bacillus</i> sp. clone CBHOS-08 (EU371582)
Landfill leachate (fresh)	LC092832	<i>Bacillus licheniformis</i> adseedstjo15	98%	<i>Bacillus licheniformis</i> LRF2X (KX364925)
Landfill leachate (fresh)	LC092833	<i>Bacillus aerius</i> rawirorabr15	99%	<i>Bacillus aerius</i> CCMMB945 (KF879282)
Landfill groundwater	LC090854	<i>Pseudomonas nitroreducens</i> szh_asesj15	98%	<i>Pseudomonas nitroreducens</i> TA-E11 (KX682023)
Landfill groundwater	LC090855	<i>Sphingopyxis</i> sp. szh_adharsh	99%	<i>Sphingopyxis</i> sp. AX-A (Jq418293)

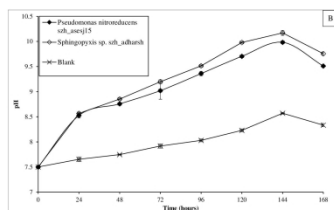
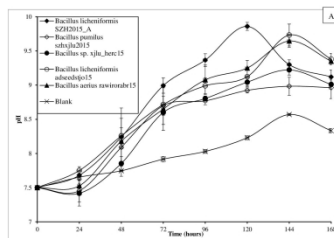


Fig 1. (A) Changes in the pH of the biomineralisation medium (along with a blank) during the growth of the bacteria isolated from groundwater. (B) Changes in the pH of the biomineralisation medium (along with a blank) during the growth of the bacteria isolated from leachate. Data points are means of experiments performed in triplicate and error bars represent the variations obtained during the pH readings.

Fig 1. (A) Changes in the pH of the biomineralisation medium (along with a blank) during the growth of the bacteria isolated from groundwater. (B) Changes in the pH of the biomineralisation medium (along with a blank) during the growth of the bacteria isolated from leachate. Data points are means of experiments performed in triplicate and error bars represent the variations obtained during the pH readings.

140x396mm (300 x 300 DPI)

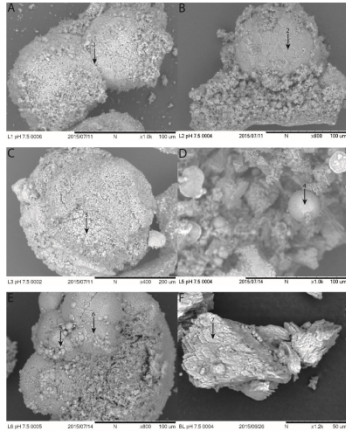


Fig 2. Spherical calcite crystals found in solutions containing (A) *Bacillus licheniformis* SZH2015_A, (1) fusing of two calcite crystals. (B) *Bacillus pumilus* szhxjlu2015, (2) fibrous patterns on the surface of a spherical calcite crystal. (C) *Bacillus* sp. xjlu_herc15, (3) very small calcite crystals (<30 μ m) on the surface of a single calcite crystal. (D) *Bacillus licheniformis* adseedstjo15, (4) single spherical calcite crystal connected with non-spherical calcite crystals. (E)

Bacillus aerius rawiorabr15, (5) small calcite crystals (50-75 μ m) fused together on the top of a calcite crystals, (6) minor cracks observed on the surface of a calcite crystals and non-spherical calcite crystal with platy overlapping layers on the surface of the calcite crystal observed in. (F) blank showing rhombohedral crystal forms.

Fig 2. Spherical calcite crystals found in solutions containing (A) *Bacillus licheniformis* SZH2015_A, (1) fusing of two calcite crystals. (B) *Bacillus pumilus* szhxjlu2015, (2) fibrous patterns on the surface of a spherical calcite crystal. (C) *Bacillus* sp. xjlu_herc15, (3) very small calcite crystals (<30 μ m) on the surface of a single calcite crystal. (D) *Bacillus licheniformis* adseedstjo15, (4) single spherical calcite crystal connected with non-spherical calcite crystals. (E) *Bacillus aerius* rawiorabr15, (5) small calcite crystals (50-75 μ m) fused together on the top of a calcite crystals, (6) minor cracks observed on the surface of a calcite crystals and non-spherical calcite crystal with platy overlapping layers on the surface of the calcite crystal observed in. (F) abiotic solution showing rhombohedral crystal forms.

143x372mm (300 x 300 DPI)

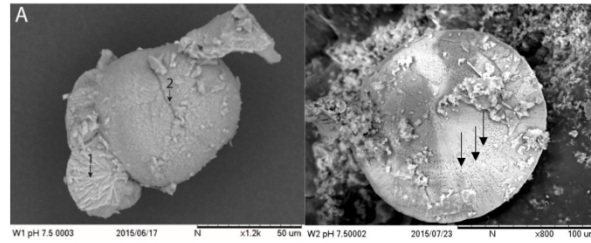


Fig 3. Scanning electron micrographs showing mineral precipitates formed in the presence of *Pseudomonas nitroreducens* szh_asesj15 (A) Radiating growth structures in the crystal (1) and internal fusing lines on a spherical calcite crystal (2). (B) Arrows indicate bacterial imprints on the surface of calcite crystals formed in the presence of *Sphingopyxis* sp. szh_adharsh.

Fig 3. Scanning electron micrographs showing mineral precipitates formed in the presence of *Pseudomonas nitroreducens* szh_asesj15 (A) Radiating growth structures in the crystal (1) and internal fusing lines on a spherical calcite crystal (2). (B) Arrows indicate bacterial imprints on the surface of calcite crystals formed in the presence of *Sphingopyxis* sp. szh_adharsh.

140x198mm (300 x 300 DPI)

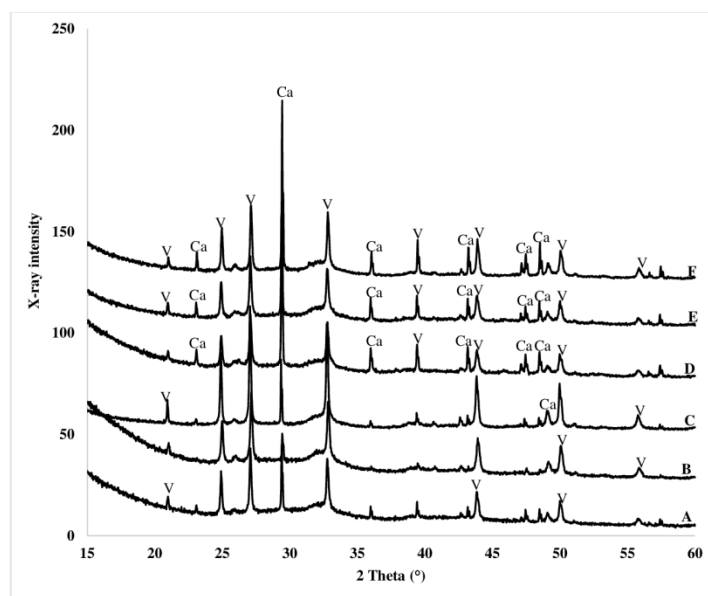


Fig 4. XRD spectra indicating multiple calcite and vaterite peaks in all five bacterial isolates and the blank. (A) *Bacillus licheniformis* SZH2015_A; (B) *Bacillus pumilus* szhxjlu2015; (C) *Bacillus* sp. xjlu_herc15; (D) *Bacillus licheniformis* adseedstjo15; (E) *Bacillus aerius* rawirorabr15 and (F) blank. (Ca= Calcite; V= Vaterite).

Fig 4. XRD spectra indicating multiple calcite and vaterite peaks in all five bacterial isolates and the blank. (A) *Bacillus licheniformis* SZH2015_A; (B) *Bacillus pumilus* szhxjlu2015; (C) *Bacillus* sp. xjlu_herc15; (D) *Bacillus licheniformis* adseedstjo15; (E) *Bacillus aerius* rawirorabr15 and (F) abiotic solution. (Ca= Calcite; V= Vaterite).

143x186mm (300 x 300 DPI)

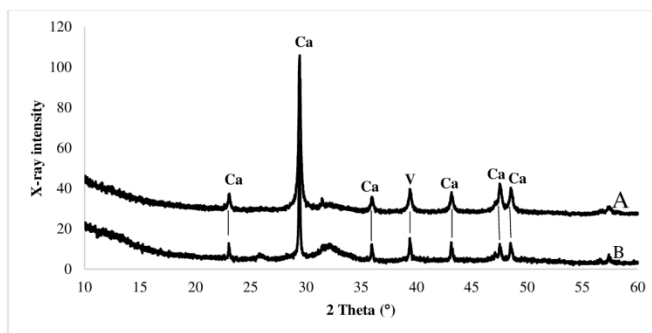


Fig 5. XRD spectra showing multiple calcites and a single vaterite peak for the bacterial samples. A = *Pseudomonas nitroreducens* szh_asesj15; B = *Sphingopyxis* sp. szh_adharsh. Ca=Calcite and V=Vaterite respectively.

Fig 5. XRD spectra showing multiple calcites and a single vaterite peak for the bacterial samples. A = *Pseudomonas nitroreducens* szh_asesj15; B = *Sphingopyxis* sp. szh_adharsh. Ca=Calcite and V=Vaterite respectively.

143x186mm (300 x 300 DPI)

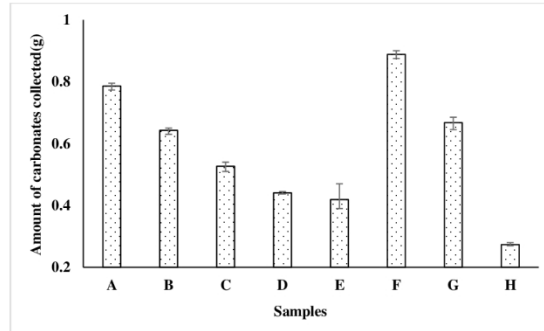


Fig 6. Calcium carbonate precipitation with error bars for individual bacterial solutions (A) *Bacillus* sp. xjlu_herc15 (B) *Bacillus licheniformis* adseedstjo15 (C) *Bacillus licheniformis* SZH2015_A (D) *Bacillus aerius* rawirorabr15 (E) *Bacillus pumilus* szhxjlu2015 (F) *Pseudomonas nitroreducens* szh_asesj15 (G) *Sphingopyxis* sp. szh_adharsh and (H) blank.

Fig 6. Calcium carbonate precipitation with error bars for individual bacterial solutions (A) *Bacillus* sp. xjlu_herc15 (B) *Bacillus licheniformis* adseedstjo15 (C) *Bacillus licheniformis* SZH2015_A (D) *Bacillus aerius* rawirorabr15 (E) *Bacillus pumilus* szhxjlu2015 (F) *Pseudomonas nitroreducens* szh_asesj15 (G) *Sphingopyxis* sp. szh_adharsh and (H) abiotic solution.

143x186mm (300 x 300 DPI)